Changes in Murine Subbasal Corneal Nerves After Scopolamine-Induced Dry Eye Stress Exposure

Cem Simsek, Takashi Kojima, Taeko Nagata, Murat Dogru, and Kazuo Tsubota

Department of Ophthalmology, Keio University School of Medicine, Tokyo, Japan

PURPOSE. To evaluate the morphologic changes in the corneal subbasal nerve (CSN) plexus in wild-type (WT) mice after exposure to scopolamine-induced dry eye stress (DES) by using in vivo confocal microscopy.

METHODS. Twenty right eyes of twenty ($n = 20$) 8-week-old WT BALB/c male mice were investigated. The mice were divided into two experimental groups; 10 eyes of 10 mice exposed to DES for 28 days and 10 eyes of 10 mice were used as a control group. All mice underwent examinations for aqueous tear secretion quantity, tear film breakup time (TBUT), corneal vital staining. and corneal sensitivity thrice (pre-experiment, 2nd week, and 4th week). CSN density, tortuosity, reflectivity, and dendritic cell (DC) densities were examined.

RESULTS. The mean aqueous tear secretion ($P < 0.0001$) and TBUTs ($P < 0.0001$) were significantly decreased after DES. The mean corneal vital staining scores were significantly higher (fluorescein, $P < 0.0001$; lissamine, $P < 0.0001$), the mean TBUTs were significantly shorter ($P < 0.0001$), and the corneal sensitivities ($P < 0.0001$) were significantly lower in the dry eye-induced mice than the control mice. The mean CSN fiber density ($P < 0.0001$) and the reflectivity ($P < 0.001$) were significantly lower; the mean tortuosity and the mean DC density were significantly higher ($P < 0.0001$) in the dry eye mice.

CONCLUSIONS. Our data demonstrated that prolonged exposure to DES resulted in alterations of CSN density; DC intensity, reflectivity, and tortuosity as well as in tear volume; TBUT; fluorescein and lissamine green staining scores; and the corneal sensitivity in WT mice.

Keywords: corneal subbasal nerves, confocal microscopy, dry eyes, scopolamine

The cornea is an intensively innervated tissue with sensory nerve fiber bundles that maintain corneal epithelial integrity and continuity.[1,2] Corneal sensory nerves originate from the ophthalmic branch of the trigeminal ganglion after penetrating the corneal stroma of the corneal limbus. In other words, the cornea is innervated on the intense aggregation of the sensory axon nerve endings called intraepithelial corneal nerves, which one constituted by corneal subbasal nerves (CSNs) and related intraepithelial nerve terminals. The intraepithelial corneal nerve endings have mechanonociceptor, polymodal nociceptor, and cold thermoreceptor functions and stimulate blinking and secreting tears over the cornea.[3]

Superficially terminating among the corneal epithelial cells, these nerve fibers are easily affected by other ocular or environmental factors.[2,4] Subbasal neuronal alterations have shown to be related to various diseases, such as neuropathic corneal ulcers, herpetic keratitis, corneal surgical interventions, diabetes mellitus, and dry eye.[5] In such cases, subbasal corneal nerves are damaged with subsequent changes, including reduction of corneal sensitivity, deterioration of corneal epithelial integrity, and decreased in epithelial cell proliferation.[6,7]

Dry eye disease (DED) has been recently described as a multifactorial chronic disease of the ocular surface characterized by tear film instability, hyperosmolarity, ocular surface inflammation, loss of homeostasis, and neurosensory abnormalities.[8] With a better understanding of the complex nature and the significant role of neuropathologic mechanisms in etiology, the association between neurosensory abnormalities and DED was emphasized in the Dry Eye Workshop II (DEWS II) report.[9] To evaluate these abnormalities, certain variables, such as CSN density, tortuosity, reflectivity and DCs, have been examined by in vivo confocal microscopy (IVCM).[10,11]

There are several dry eye mouse models investigating the pathogenesis of DED without considering the subbasal neuronal alterations in dry eye mouse models.[12] In our previous experimental study, we generated a short-term dry eye mouse model that mimicked the dry eyes in visual display terminal workers. We called it "the environmental dry eye stress (EDES) model" in which we observed a reduction in CSN density and an increase in dendritic cell (DC) numbers.[13] However, there is paucity of knowledge in relation to the effects of longer dry conditions on corneal nerves.

In the current study, we aimed to evaluate the morphologic alterations and branch patterns of the CSN plexus in the wild-type (WT) mice exposed to long-term dry eye stress by IVCM.

MATERIALS AND METHODS

Animals and Micro-Osmotic Pump (MOP) Implantation

Twenty right eyes of 20 ($n = 20$) 8-week-old WT BALB/c male mice (27–31 g body weight; CLEA, Osaka, Japan) were used for this study. Animals were divided into two experimental groups, namely, 10 eyes of 10 mice exposed to dry eye stress ($n = 10$)

615

for 28 days and 10 eyes of 10 mice used as a control group ($n = 10$). Sample size calculation for this research study was done according to the G-Power statistical power analyses program (Heinrich, Düsseldorf University, Germany) by specifying input parameters, including the type 1 error, effect size, and standard deviation.[14] To deliver the DES, the mice were shaved from their back and Alzet MOPs (Model 1002; Durect Corp., Cupertino, CA, USA) were implanted subcutaneously just above their tails for 28 days. The MOP releases prepared solutions nonstop for 2 weeks without the need for external intervention or often handling of the animals. For subcutaneous placement, a minimal incision was performed under the skin between the muscle tissue. A microcompartment was created by dissecting the subcutaneous connective tissue apart with Vannas scissors. The MOP was inserted through the incisions that were then sutured with three nonresorbable sutures. The MOP was replaced with a new one on the 15th day of the experiment with the same protocol because the pump life was 14 days. An absolute sterile technique was used throughout the infilling, interference, and surgical implantation procedure of the MOP.

Filling MOP With Scopolamine

The MOP has a 0.21 ± 0.01 μL/h mean pumping rate with 100 μl of reservoir volume that can last for 14 days of pumping. To form DES, 10 mice were infused with 0.2 mg/kg/day scopolamine (dissolved in PBS) per day and 10 mice were infused with PBS solution as the control group. To avoid unpredictable pumping rate fluctuations, each pump was filled completely without trapped air bubbles with a small syringe (1.0 mL). All experimental procedures were performed under a fixed room temperature ($25 \pm 3°C$) and humidity ($24\% \pm 4\%$). All studies were performed in accordance with the Association for Research in Vision and Ophthalmology Statement for the Use of Animals in Ophthalmic and Vision Research. The Animal Experimentation Ethics Committee of the Keio University School of Medicine approved the current research procedures.

Corneal Sensation Assessment

We used a modified Cochet Bonnet aesthesiometer according to the previous reports.[15] Corneal sensitivity assessment was performed thrice: pre-experiment, 2nd week, and 4th week of the experiment. Hi Loop 0.3 nylon filaments (Unitika Ltd., Tokyo, Japan), which had a 0.09-mm diameter, were used to evaluate the corneal sensitivity in all mice. Seven filaments ranging from 0.5 to 4 cm in length were prepared by attaching them to a holder. Starting from the longest filament (4 cm, the lowest pressure), each length of nylon filament was applied three times by stimulating the corneal nerves to cause a corneal blink response. The filament contacted the central cornea perpendicularly, avoiding contact with the eyelashes and lid margins. The nylon filament length was shortened by 5-mm increments until the mouse demonstrated a complete blink reflex. This procedure was applied to the central cornea of both eyes under magnifying glasses without any light source. Three measurements were recorded at each time point, and the average value was applied for analysis. The high repeatability of corneal sensation values was confirmed before the experiment.

Aqueous Tear Secretion Quantity, Tear Film Breakup Time (TBUT), and Ocular Surface Vital Staining Assessments

All mice underwent examinations for aqueous tear secretion quantity, TBUT, and corneal vital staining at three time points (pre-experiment, 2nd week, and 4th week). Aqueous tear secretion quantity, TBUT, and corneal vital staining were performed according to protocols described in our previous study.[13] Briefly, aqueous tear secretion quantity was evaluated by phenol red-impregnated cotton threads (Zone-Quick; Showa Yakuhin Kako Co., Ltd., Tokyo, Japan) without anesthesia. We placed the cotton threads into the lateral canthus with microforceps for 30 seconds. The wet length of the cotton threads was measured with a ruler provided by the manufacturer in millimeters.

TBUT was examined to assess the ocular surface tear film stability. Initially, one drop of 1 μL of 2% sterile fluorescein (FL) was applied onto the ocular surface of the mouse by a micropipette. Excess FL was wiped from the lateral canthus. After a natural blink response stimulated by air puff by using 1-mL syringe, the TBUT was examined with portable slit-lamp biomicroscopy by using cobalt blue light (Kowa Co., Ltd., Tokyo, Japan) three times, and the mean of these results was then calculated.

FL and lissamine green (LG) staining were examined 2 minutes after TBUT assessment by using a scoring system previously described by Shimmura et al.[16] The cornea was divided into three parts (superior, middle, and inferior), and each part was scored between 0 and 3 points according to the extent of the area stained. A score of 0 signified no staining, 1 signified mild staining, 2 signified moderate staining, and 3 signified severe staining for a minimum and maximum total score of 0 and 9 points, respectively. Five microliters of PBS was used to wash out FL, which was removed from the lateral canthus before repeating the same procedure with the LG dye. Vital staining photographs were recorded in JPEG format by using a microscope connected to a digital camera with the same settings maintained for all mice.

In Vivo Laser Scanning Microscopic Assessment and Analysis of Images

We performed ocular surface confocal analyses by in vivo laser scanning confocal microscopy with an anterior segment adaptor. The Rostock Cornea Module of the Heidelberg Retinal Tomograph II (HRT) (Heidelberg Engineering, Heidelberg, Germany) was used to examine the corneal morphologic alterations. Following intraperitoneal anesthesia injection (4 mg/mL of xylazine and 6 mg/mL of ketamine), a carbomer 2% gel (comfort gel, Dr. Mann Pharma; Fabrik GmbH, Berlin, Germany) was applied to the cornea to avoid exposure and dryness during IVCM examination. The laser source, internally mounted in the HRT, provides a 670-nm red wavelength diode laser. High-resolution real-time images obtained by IVCM consisted of 384×384 pixels covering an area of 400×400 μm (horizontal × vertical) with a lateral resolution of 1 μm/pixel. The images were recorded as a JPEG frame with a resolution of 8 bits of data and a 128-bit binary floating-point format. Six to eight complete sequences, each containing 100 images, were recorded from each cornea (each frame representing an area of 160.00 μm^2), and the approximate duration of IVCM examination was 8 minutes per eye. Four nonoverlapping representative images of each cornea were selected for corneal morphologic analysis. As previously described,[13] two masked experienced researchers analyzed the well-focused images for corneal nerve morphologic features and investigated the density of nerve fibers (NFD), tortuosity and reflectivity of CSN, and DC density as follows:

1. The NFD was assessed by measuring the total length of CSN fibers within a frame (160,000 μm^2), as defined in our previous study.[13] After semiautomatically marking the CSN in each frame, the NFD was automatically
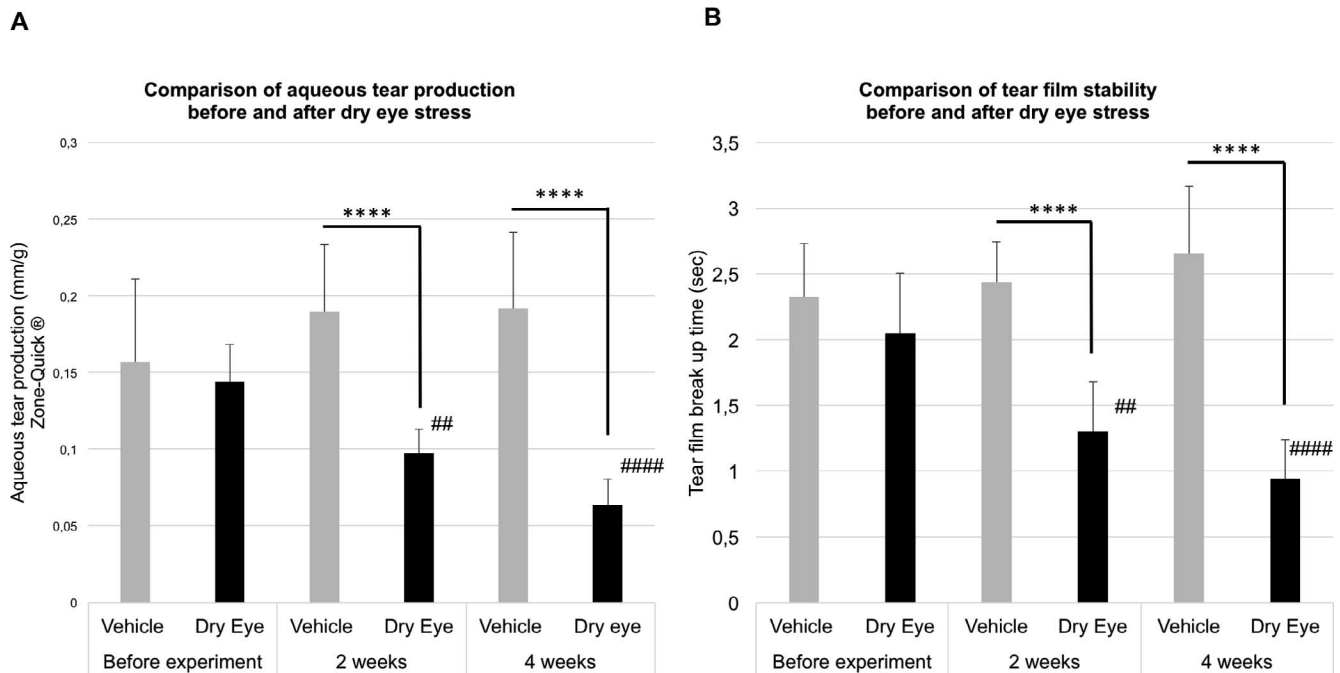
A

B

FIGURE 1. Graphs showing aqueous tear production and tear film stability results. (**A**) A marked decrease in aqueous tear quantity can be seen in the BALB/c mice after 2 weeks ($P < 0.0001$) and 4 weeks ($P < 0.0001$) of DES application. (**B**) Comparison of the mean TBUT after 2 and 4 weeks of DES application; the mean TBUT in the non-DED group was significantly longer than that in the DED group ($P < 0.0001$). The hash symbol (#) represents comparison between pre-experiment and other time points. #$P < 0.05$, ##$P < 0.01$, ###$P < 0.001$, ####$P < 0.0001$. The asterisk symbol (*) represents comparison between treatment groups. *$P < 0.05$, **$P < 0.01$, ***$P < 0.001$, ****$P < 0.0001$.

measured by the NeuronJ plug-in for ImageJ software (http://rsb.info.nih.gov/ij/; provided in the public domain by National Institutes of Health, Bethesda, MD, USA). Four different representative images for each cornea were analyzed in pixels. The mean CSN for each cornea was calculated by averaging these total values. The data were determined as density ($\mu m/mm^2$).

2. The CSN nerve tortuosity was evaluated at the subbasal layer relating to a previous grading scale. The grading scales consisted of a series of images derived from our and other previous studies of corneal innervation using confocal microscopy. Oliveira-Soto et al.[17] classified human corneal nerve tortuosity into five grades. Likewise, in our previous study, we classified mice corneal nerve tortuosity according to subbasal nerve curve magnitude and divided it into five grades from 0 to 5.[13]

3. The grading of nerve reflectivity was also performed according to our previous research.[13] In that study, we classified mice corneal nerve reflectivity into five grades from 0 (no effect) to 5 (strong effect). Similarly, only the nerves longer than 50% of the width frame underwent reflectivity assessment.[13]

4. The images were also examined for the density of DCs. DCs were morphologically identified through bright cellular images with a branching dendritic morphology located at the level of subbasal nerve plexus layer. Four representative images were used to evaluate the density of epithelial DCs.

Statistical Analysis

To analyze the effects of two factors, including time points and dry eye stress, the 2-way repeated measures ANOVA test was performed to compare tear quantity, vital staining scores, corneal sensation, and CSN parameters at different time points. The Tukey's test was performed as a multiple comparison test (post hoc test). A P value less than 5% was considered to be statistically significant.

RESULTS

Aqueous Tear Secretion Quantity Alterations

Weight-adjusted aqueous tear production quantity, the mean TBUT, and corneal vital staining score alterations were measured three times during the experiments: before the experiments, 2nd week, and 4th week of the experiments. The mean tear production values for the control group (non-DED group) were 0.156 ± 0.05 before the experiment, 0.189 ± 0.04 mm/g at the 2nd week of the experiment, and 0.191 ± 0.04 mm/g at the 4th week of experiment. The mean tear production values for DED group were 0.143 ± 0.02 before the experiment, 0.097 ± 0.01 at 2 weeks of the experiment, and 0.063 ± 0.01 mm/g at 4 weeks of the experiment. Compared with the control group (non-DED), the DED mice demonstrated a significant decrease at the 2nd ($P = 0.0081$) and 4th ($P < 0.0001$) week of the experiment in tear volume after exposure to DES (Fig. 1A). At both two and four weeks after exposure to dry eye stress, the mean tear secretion quantity in the DED group was significantly lower than the control group (both time points, $P < 0.0001$).

TBUT and Ocular Surface Vital Staining Score Alterations

The mean TBUTs for the control group (non-DED) were 2.32 ± 0.40 before the experiment, 2.43 ± 0.30 at the 2nd week of the experiment, and 2.65 ± 0.50 seconds at the 4th week of the experiment. The mean TBUTs in the DED group were
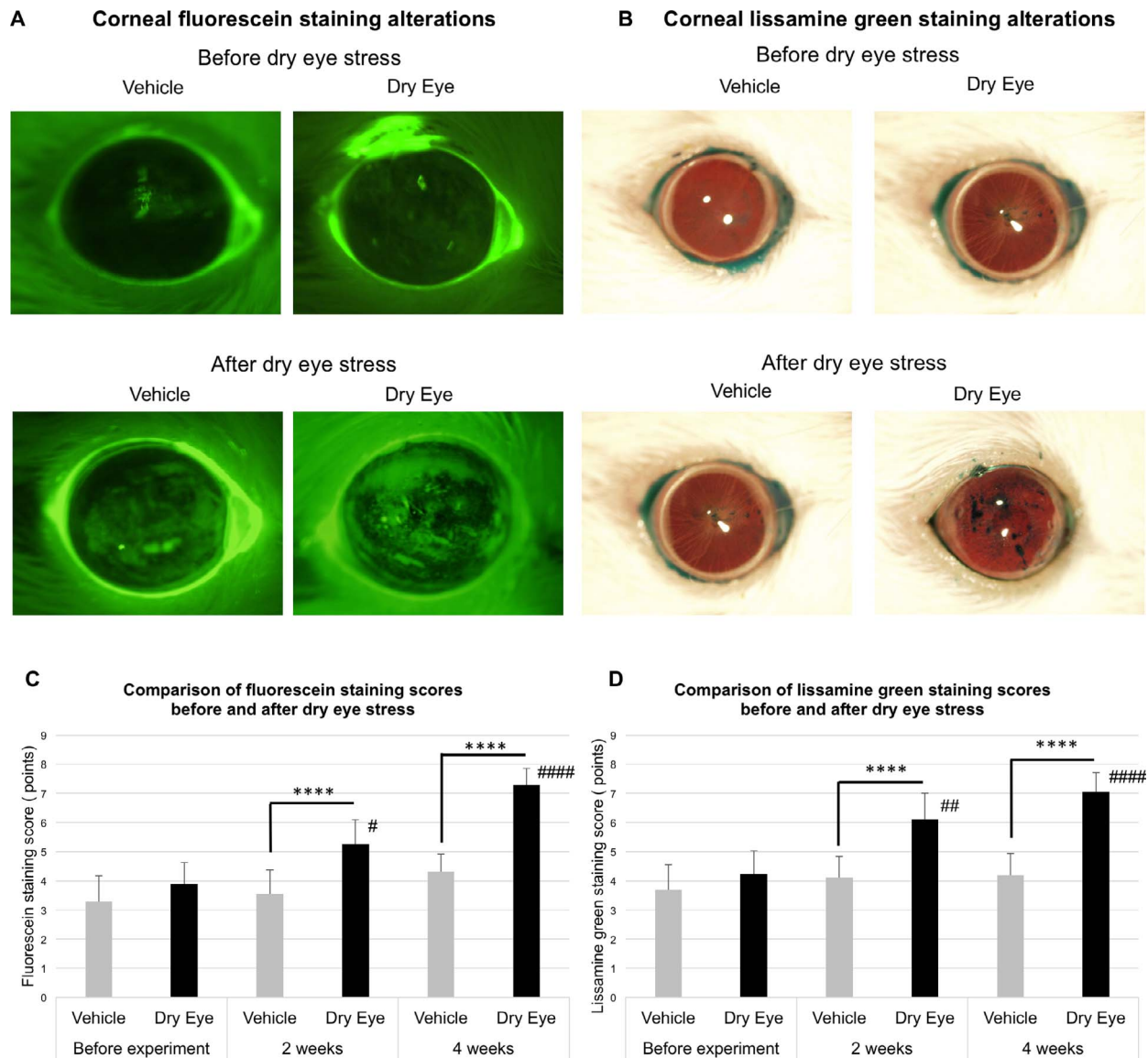
FIGURE 2. Representative anterior segment photographs and comparison of corneal FL and LG staining scores in the vehicle (non-DED) and the DES-applied mice group. Anterior segment photographs of FL and LG staining before and after DES are shown. Note a marked deterioration in the FL and LG staining scores in the dry eye group compared to the vehicle (non-DED) after DES exposure (**A, B**). (**C**) The mean FL staining score in the DED group significantly increased after DES exposure at 2nd ($P < 0.0001$) and 4th week ($P < 0.0001$). (**D**) Please note a significant increase of LG staining scores in the dry eye group compared to the vehicle (non-DED) after DES exposure (2nd week, $P < 0.0001$; 4th week, $P < 0.0001$). The hash symbol (#) represents comparison between pre-experiment and other time points. #$P < 0.05$, ##$P < 0.01$, ###$P < 0.001$, ####$P < 0.0001$. The asterisk symbol (*) represents comparison between treatment groups. *$P < 0.05$, **$P < 0.01$, ***$P < 0.001$, ****$P < 0.0001$.

2.05 ± 0.45 before the experiment, 1.30 ± 0.37 at the 2nd week of the experiment, and 0.94 ± 0.29 sec at 4th week of experiment. The mean TBUT in the DED group showed a significant decrease at the 2nd ($P = 0.0019$) and 4th ($P < 0.0001$) week of the experiment after exposure to DES (Fig. 1B). At both 2 and 4 weeks after exposure to dry eye stress, the mean TBUT in the DED group was significantly shorter than the control group (both time points, $P < 0.0001$).

We also investigated the changes in corneal vital staining scores before the experiment, at the 2nd and 4th week of the experiment. The mean FL staining scores did not show any significant difference in the control group (3.3 ± 0.86 before experiment versus 4.3 ± 0.60 points after four weeks, $P = 0.68$). The mean FL staining scores increased significantly from 3.9 ± 0.71 to 7.27 ± 0.57 points after exposure to 4 weeks of DES ($P < 0.0001$) (Fig. 2A). The LG staining scores did not

show any significant difference in the control group (3.7 ± 0.85 before the experiment versus 4.1 ± 0.63 points after the 4th week, $P = 0.53$). The LG staining scores elevated significantly from 4.25 ± 0.78 to 7.05 ± 0.63 points after exposure to 4 weeks of DES ($P < 0.0001$) (Fig. 2B). The mean FL and LG staining scores in the DES group were significantly higher than the control group (non-DED) at both the 2nd and 4th week (FL staining, $P < 0.0001$; LG staining, $P < 0.0001$).

Corneal Sensitivity Alterations

Corneal sensitivity in the DES group was significantly lower than the control group at the 2nd week and 4th week of the experiment (2nd week results, 3.5 ± 0.40 in control group (non-DED) versus 2.72 ± 0.30 mm in DED group, $P < 0.0001$; 4th week results, 3.5 ± 0.30 in control group versus $2.1 \pm$
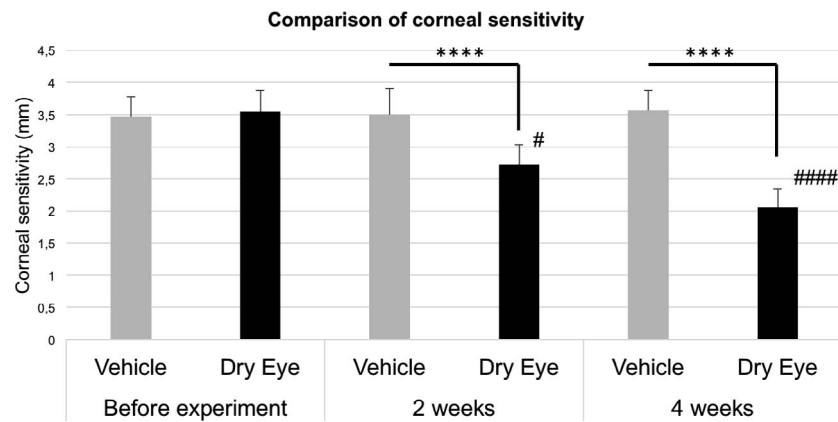
FIGURE 3. Corneal sensitivity is decreased in response to DES. Please note the significant decrease in the corneal sensitivity in the dry eye group after DES exposure at 2nd and 4th week ($P < 0.0001$ for both). The corneal sensitivity in the vehicle group (non-DED) is significantly higher than that in the dry eye group after DES exposure ($P < 0.0001$). The hash symbol (#) represents comparison between pre-experiment and other time points. #$P < 0.05$, ##$P < 0.01$, ###$P < 0.001$, ####$P < 0.0001$. The asterisk symbol (*) represents comparison between treatment groups. *$P < 0.05$, **$P < 0.01$, ***$P < 0.001$, ****$P < 0.0001$.

0.29 mm in DED group, $P < 0.0001$). Additionally, corneal sensitivity values at both 2 and 4 weeks after exposure to dry eye stress significantly decreased (2 weeks, $P = 0.014$; 4 weeks, $P < 0.0001$). On the other hand, no remarkable change was found in the corneal sensitivity values in the control group before and after the experiment ($P = 0.934$) (Fig. 3).

IVCM Results

To investigate whether BALB/c mice also demonstrated any alterations in CSN morphology with DES, we compared CSN density, tortuosity, reflectivity, and DC density between two time points: pretreatment and 4 weeks after exposure to dry eye stress. To assess the effect of DES, a total of 156 images containing 1067 nerves were evaluated for NFD by two experienced researchers (Fig. 4). IVCM assessment for NFD was performed under anesthesia. The mean NFD was 2722 ± 596 in the control (non-DED) group and 2493 ± 208 pixels/frame in the DES group. The data showed that there was no significant change in NFD before the experiment between the two groups ($P = 0.38$). On the other hand, there was a statistically significant decrease in the mean NFD in the DES group after 4 weeks of the experiment ($P = 0.0038$). After exposure to 28 days of DES, the mean NFD became 2538 ± 933 in the control (non-DED) group and 1570 ± 506 pixels/frame in the DES group. The mean NFD at 4 weeks after exposure to dry eye stress was significantly lower in the DES group than in the control group ($P < 0.0001$) (Fig. 5A).

To investigate the tortuosity and reflectivity, 436 nerves from 156 images were investigated using our previously defined grading scale. The mean subbasal nerve tortuosity values were as follows: before experiment control group, 0.52 ± 0.22; before experiment DES group, 0.59 ± 0.15; after 4 weeks of experiment control group, 0.46 ± 0.22; and after 4 weeks of experiment DES group, 1.09 ± 0.25. After exposure to 4 weeks of scopolamine, the mean subbasal nerve tortuosity grades decreased significantly in the DES group ($P < 0.0001$). Furthermore, after 4 weeks of experiment, there was a statistically significant difference in the tortuosity values between the control group and the DES group ($P < 0.0001$). There was no significant difference in the tortuosity values in the control group before and after the experiment ($P = 0.637$) (Fig. 5B).

The mean CSN reflectivity grade values were as follows: before experiment control group, 1.53 ± 0.26; before

experiment DES group, 1.58 ± 0.36; after 4 weeks of experiment control group, 1.6 ± 0.22; and after 4 weeks of experiment DES group, 1.26 ± 0.28. After exposure to 4 weeks of scopolamine, the mean subbasal nerve reflectivity grades decreased significantly in the DES group ($P = 0.011$). Moreover, after 4 weeks of experiment there was a statistically significant difference in the mean reflectivity values between the control group and the DES group ($P = 0.0028$). There was no significant difference in reflectivity values in the control group before and after the experiment ($P = 0.765$) (Fig. 5C).

The DC density in the control group (8.25 ± 3.59 cells/mm^2) was significantly lower than that in the DES group (14.57 ± 4.99 cells/mm^2) after 4 weeks of experiment ($P = 0.0013$). Additionally, there was a significant difference in the DC densities in the DES group before (9.18 ± 4.49) and after the experiment ($P = 0.0257$) (Fig. 5D).

DISCUSSION

CSNs play an essential role in maintaining ocular surface health and vision as a result of preserving corneal integrity and sensation.[5] Recently, IVCM has become a widely used noninvasive diagnostic tool for the clinical evaluation of the cornea, which ensures high-resolution images of corneal nerves, structures, and layers.[10] Jiang et al.[18] reported that noninvasive IVCM imaging of CSN is a practical and useful method to determine the alterations of small fiber neuropathy. Because previous studies have reported a high agreement in the evaluation of corneal nerves between IVCM and histologic examinations, IVCM has been used to evaluate qualitative and quantitative variations of the corneal nerves in many conditions, including herpes zoster ophthalmicus, corneal transplantation, laser refractive surgery (laser-assisted epithelial keratomileusis and photorefractive keratectomy), noncorneal ocular procedures (cataract surgery, laser panretinal photocoagulation, laser retinopexy, and scleral buckles), antiglaucoma medical therapy (particularly topical beta-adrenergic antagonists), aging, diabetes mellitus, and dry eye.[19-29] A significant decrease in CSN density has been shown nearly in all of these conditions. Most of the studies investigating corneal nerves in DED patients also mainly assessed the CSN density and found a decrease in the majority, whereas others found an increase or no change.[30-33] These variable results were found to be associated with differences in DED severity, corneal nerve damage severity, neural regeneration/degenerative patterns,

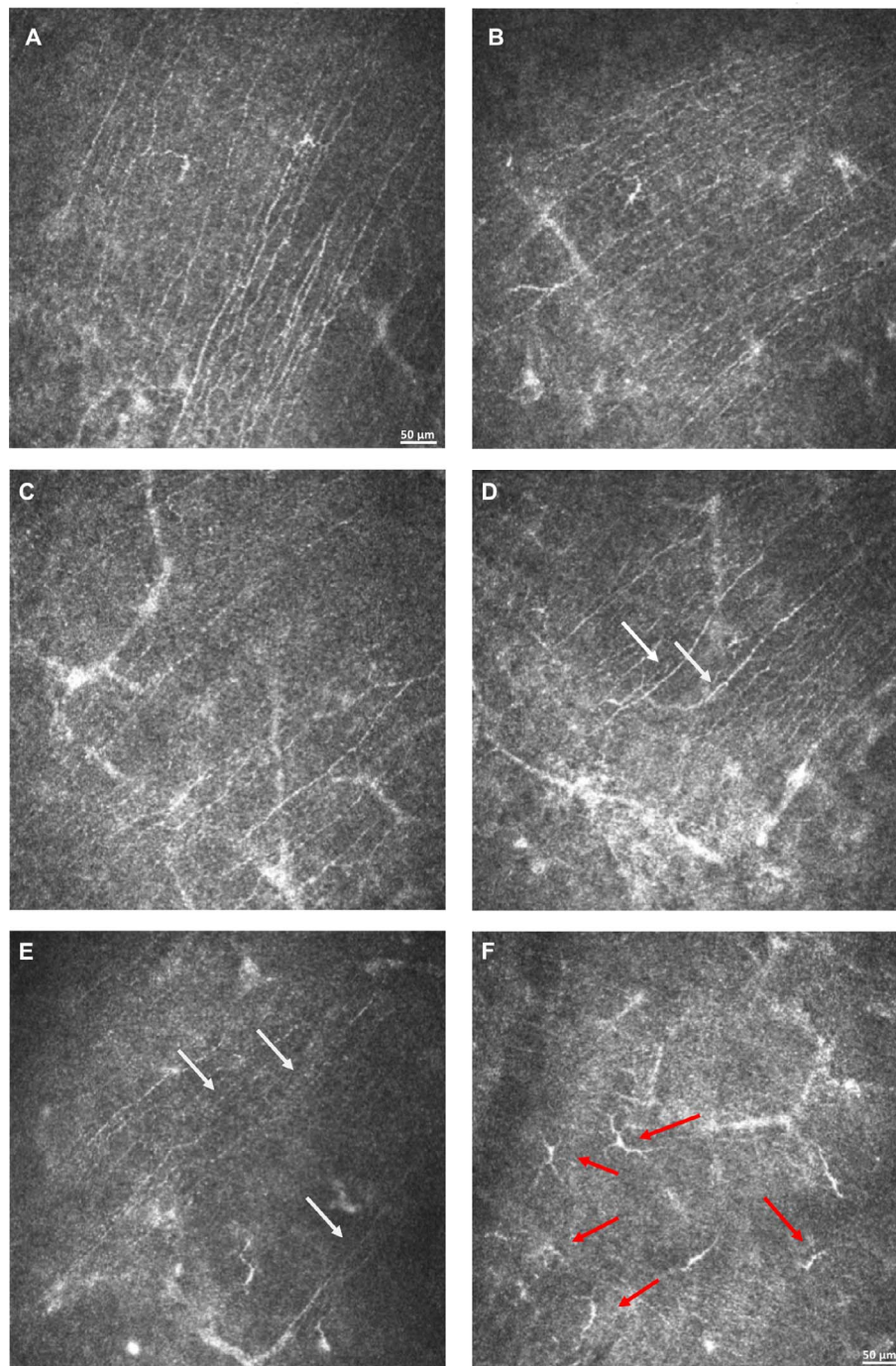**Subbasal corneal nerves and DCs comparison IVCM images**

FIGURE 4. Comparison of in vivo confocal microscopy images in the vehicle (non-DED) and DES (DED)-applied group. Representative IVCM images of BALB/c male mice before and after 28 days of DES. (**A**) Baseline representative IVCM image of vehicle (non-DED) group before dry eye stress. (**B**) Representative IVCM image of vehicle (non-DED) after dry eye stress. (**C**) Baseline representative image of dry eye (scopolamine) group before dry eye stress. (**D**) Significant increase in nerve tortuosity can be seen after 28 days of scopolamine application. *White arrow* indicates the increased nerve tortuosity. (**E**) Significant reduction in CSN fibers can be seen. Reduced CSNs indicated by *white arrows*. (**F**) Significant increase in DCs can be seen clearly. *Red arrows* indicate the DCs.

and inflammation levels.[13] Recently, Stepp et al.[34] have demonstrated that decreased intraepithelial corneal nerves in the CD25 null Sjögren syndrome mouse model is accompanied by reduced corneal sensitivity and increased corneal epithelial cell proliferation. Furthermore, Stepp et al.[35] reported a significant decrease in axon thickness, density, and apical extension of the intraepithelial nerve terminals after 5 days of dry eye exposure in C57BL/6 mice. Additionally, a previous
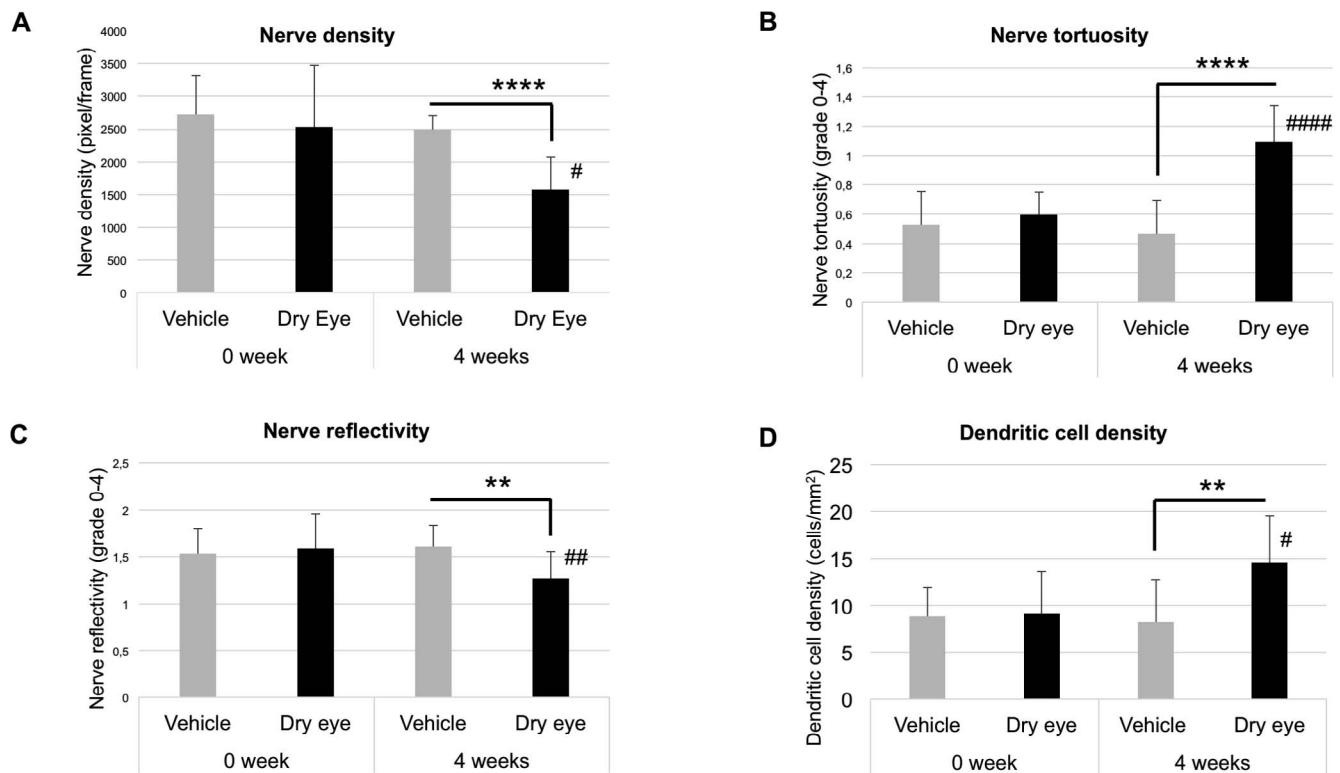
FIGURE 5. Quantitative analysis of in vivo confocal microscopy images for the nerve density, tortuosity, reflectivity, and DC density. Graphs showing a significant reduction of nerve density (**A**, $P < 0.0001$) and nerve reflectivity (**C**, $P < 0.01$) in the dry eye group compared to the vehicle (non-dry) group. A significant increase of nerve tortuosity (**B**, $P < 0.0001$) and DC density (**D**, $P < 0.01$) in the dry eye group compared to the vehicle (non-dry) group after 28 days of DES exposure. The hash symbol (#) represents comparison between time points. #$P < 0.05$, ##$P < 0.01$, ###$P < 0.001$, ####$P < 0.0001$. The asterisk symbol (*) represents comparison between treatment groups. *$P < 0.05$, **$P < 0.01$, ***$P < 0.001$, ****$P < 0.0001$.

study done by De Paiva et al.[36] has shown acute deterioration of barrier function and increased inflammation even after 5 days of desiccating stress in mice. Similarly, we found a notable decrease in subbasal nerve density after acute environmental stress in our previous study.[13] In the current study, 28 days of dry eye stress reduced CSN density in the WT mice.

In previous dry eye studies, besides CSN density, other morphologic parameters, including tortuosity, reflectivity, DC density, and beading pattern, have been also been evaluated with variable results (related to neural regenerations).[37–40] Most of these human studies performed in patients with dry eye have shown an increase in DC density and alterations in other parameters due to the consequence of neural regeneration after CSN deterioration[19,29,39,41] and these alterations were associated with clinical symptoms.[42] Furthermore, neurotransmitters and neuropeptides, such as vasoactive intestinal polypeptide, pituitary adenylate cyclase-activating peptide, and calcitonin gene-related peptide, induced by the main corneal nerve fibers regulate the function of DC in DED.[32,33] It has been well demonstrated that inflammation stimulated by both innate and adaptive immune responses is critical to pathogenesis and the chronicity of DED.[43,44] In the current study, we also found an increase in DC density in WT mice after exposure to dry eye stress, as found in our previous environmental acute stress study.[13]

As for tortuosity and reflectivity, the results were different between acute and longer term stress conditions. In this study, we found an increase in tortuosity and decrease in reflectivity after exposure to dry eye stress, whereas these parameters were stable in our previous acute EDES study.[13] Recently, a dry eye study comparing CSN tortuosity and reflectivity between dry eye patients and controls also has found an increase in tortuosity and a reduction in nerve reflectivity in the dry eye patients.[45] An increase in tortuosity in chronic stress was considered to be associated with neural regenerations, as demonstrated in previous studies on chronic diseases, such as diabetic neuropathy,[46,47] keratoconus,[48] Sjögren's syndrome,[49] DED,[30,40] and meibomian gland dysfunction,[38,39] and our results were consistent with these studies.

Moreover, in this study, we also evaluated tear volume, TBUT, FL staining scores, LG staining scores, and corneal sensitivity changes after DES exposure. Both acute and longer term dry eye stress showed a similar level of decreased tear secretion quantity. We observed a significant increase in FL and LG staining and decrease in tear volume and TBUT as expected. Corneal sensitivity threshold examination demonstrated that corneal sensitivity was reduced after application of dry eye stress. According to our hypotheses, corneal sensitivity was reduced due to decreased CSN density. This can be explained by the pathologic changes that occur in the corneal epithelium, which are the result of reduced tear volume. Xu et al.[50] also found a negative correlation between corneal sensitivity and rose bengal/FL staining scores.

This study has several limitations, including the use of only male mice (to avoid hormonal changes of menstrual cycle). Furthermore, we did not observe how the nerves healed after longer term DES. Further studies should be performed to evaluate the chronic effect of DES. In this study, we used the BALB/c mice strain because CSN density is higher in BALB/c mice compared with same-aged C57BL/6 mice.[51] Further studies should also focus on female mice and different mouse strains. In this study, we evaluated the alterations of DC

density. Although DCs were carefully identified by two examiners through bright cellular images with branching dendritic morphology, they were not phenotypically determined as DCs. Further study using immunohistochemistry should be performed to confirm our current results.

In the human study, it is difficult to examine the sole effect of dry eye on the corneal nerve because the influence of the systemic diseases and external factors cannot be excluded. Therefore, there are discrepancies in reporting nerve alterations between DE studies as described above. In this respect, conducting research by using a dry eye animal model is essential for understanding the pathophysiology. The novelty of this study is that we observed in vivo alterations in the subepithelial nerve plexus after scopolamine-induced dry eye stress in a mouse model. This study may form the basis of future research to evaluate the dry eye treatment drugs and elucidate the pathophysiology of the disease.

In conclusion, prolonged exposure to DES in WT mice resulted in significant changes in CSN density, DC intensity, reflectivity, and tortuosity as well as in tear volume TBUT, FL-LG staining scores, and corneal sensitivity.

Acknowledgments

References

1. Muller LJ, Marfurt CF, Kruse F, Tervo TM. Corneal nerves: structure, contents and function. *Exp Eye Res*. 2003;76:521–542.

2. Marfurt CF, Cox J, Deek S, Dvorscak L. Anatomy of the human corneal innervation. *Exp Eye Res*. 2010;90:478–492.

3. Gonzalez-Gonzalez O, Bech F, Gallar J, Merayo-Lloves J, Belmonte C. Functional properties of sensory nerve terminals of the mouse cornea. *Invest Ophthalmol Vis Sci*. 2017;58:404–415.

4. Guthoff RF, Wienss H, Hahnel C, Wree A. Epithelial innervation of human cornea: a three-dimensional study using confocal laser scanning fluorescence microscopy. *Cornea*. 2005;24:608–613.

5. Yang AY, Chow J, Liu J. Corneal innervation and sensation: the eye and beyond. *Yale J Biol Med*. 2018;91:13–21.

6. Yamaguchi T, Turhan A, Harris DL, et al. Bilateral nerve alterations in a unilateral experimental neurotrophic keratopathy model: a lateral conjunctival approach for trigeminal axotomy. *PLoS One*. 2013;8:e70908.

7. Ferrari G, Ueno H, Bignami F, Rama P, Dana R. Trigeminal stereotactic electrolysis induces dry eye in mice. *Acta Ophthalmol*. 2013;91:e162–e163.

8. Tsubota K, Yokoi N, Shimazaki J, et al. New perspectives on dry eye definition and diagnosis: a consensus report by the Asia Dry Eye Society. *Ocul Surf* 2017;15:65–76.

9. Craig JP, Nelson JD, Azar DT, et al. TFOS DEWS II report executive summary. *Ocul Surf*. 2017;15:802–812.

10. Parissi M, Karanis G, Randjelovic S, et al. Standardized baseline human corneal subbasal nerve density for clinical investigations with laser-scanning in vivo confocal microscopy. *Invest Ophthalmol Vis Sci*. 2013;54:7091–7102.

11. Cruzat A, Pavan-Langston D, Hamrah P. In vivo confocal microscopy of corneal nerves: analysis and clinical correlation. *Semin Ophthalmol*. 2010;25:171–177.

12. Park YS, Gauna AE, Cha S. Mouse models of primary Sjogren's syndrome. *Curr Pharm Des*. 2015;21:2350–2364.

13. Simsek C, Kojima T, Dogru M, Tsubota K. Alterations of murine subbasal corneal nerves after environmental dry eye stress. *Invest Ophthalmol Vis Sci*. 2018;59:1986–1995.

14. Faul F, Erdfelder E, Lang AG, Buchner A. G*Power 3: a flexible statistical power analysis program for the social, behavioral, and biomedical sciences. *Behav Res Methods*. 2007;39:175–191.

15. Yamazaki R, Yamazoe K, Yoshida S, et al. The semaphorin 3A inhibitor SM-345431 preserves corneal nerve and epithelial integrity in a murine dry eye model. *Sci Rep*. 2017;7:15584.

16. Shimmura S, Ono M, Shinozaki K, et al. Sodium hyaluronate eyedrops in the treatment of dry eyes. *Br J Ophthalmol* 1995;79:1007–1011.

17. Oliveira-Soto L, Efron N. Morphology of corneal nerves using confocal microscopy. *Cornea*. 2001;20:374–384.

18. Jiang MS, Yuan Y, Gu ZX, Zhuang SL. Corneal confocal microscopy for assessment of diabetic peripheral neuropathy: a meta-analysis. *Br J Ophthalmol*. 2016;100:9–14.

19. Alhatem A, Cavalcanti B, Hamrah P. In vivo confocal microscopy in dry eye disease and related conditions. *Semin Ophthalmol*. 2012;27:138–148.

20. De Cilla S, Fogagnolo P, Sacchi M, et al. Corneal involvement in uneventful cataract surgery: an in vivo confocal microscopy study. *Ophthalmologica*. 2014;231:103–110.

21. Erie JC, McLaren JW, Hodge DO, Bourne WM. Recovery of corneal subbasal nerve density after PRK and LASIK. *Am J Ophthalmol*. 2005;140:1059–1064.

22. Erie JC, McLaren JW, Hodge DO, Bourne WM. The effect of age on the corneal subbasal nerve plexus. *Cornea*. 2005;24:705–709.

23. Hamrah P, Cruzat A, Dastjerdi MH, et al. Unilateral herpes zoster ophthalmicus results in bilateral corneal nerve alteration: an in vivo confocal microscopy study. *Ophthalmology*. 2013;120:40–47.

24. Misra S, Ahn HN, Craig JP, Pradhan M, Patel DV, McGhee CN. Effect of panretinal photocoagulation on corneal sensation and the corneal subbasal nerve plexus in diabetes mellitus. *Invest Ophthalmol Vis Sci*. 2013;54:4485–4490.

25. Neira-Zalentein W, Holopainen JM, Tervo TM, et al. Corneal sensitivity in diabetic patients subjected to retinal laser photocoagulation. *Invest Ophthalmol Vis Sci*. 2011;52:6043–6049.

26. Niederer RL, Perumal D, Sherwin T, McGhee CN. Corneal innervation and cellular changes after corneal transplantation: an in vivo confocal microscopy study. *Invest Ophthalmol Vis Sci*. 2007;48:621–626.

27. Niederer RL, Perumal D, Sherwin T, McGhee CN. Age-related differences in the normal human cornea: a laser scanning in vivo confocal microscopy study. *Br J Ophthalmol*. 2007;91:1165–1169.

28. Van Went C, Alalwani H, Brasnu E, et al. Corneal sensitivity in patients treated medically for glaucoma or ocular hypertension [in French]. *J Fr Ophtalmol*. 2011;34:684–690.

29. Villani E, Baudouin C, Efron N, et al. In vivo confocal microscopy of the ocular surface: from bench to bedside. *Curr Eye Res*. 2014;39:213–231.

30. Benitez del Castillo JM, Wasfy MA, Fernandez C, Garcia-Sanchez J. An in vivo confocal masked study on corneal epithelium and subbasal nerves in patients with dry eye. *Invest Ophthalmol Vis Sci*. 2004;45:3030–3035.

31. Bron AJ, de Paiva CS, Chauhan SK, et al. TFOS DEWS II pathophysiology report. *Ocul Surf*. 2017;15:438–510.

32. Choi EY, Kang HG, Lee CH, et al. Langerhans cells prevent subbasal nerve damage and upregulate neurotrophic factors in dry eye disease. *PLoS One*. 2017;12:e0176153.

33. He J, Cortina MS, Kakazu A, Bazan HE. The PEDF neuroprotective domain plus DHA induces corneal nerve regeneration

Investigative Ophthalmology & Visual Science

after experimental surgery. *Invest Ophthalmol Vis Sci*. 2015; 56:3505–3513.

34. Stepp MA, Pal-Ghosh S, Tadvalkar G, Williams AR, Pflugfelder SC, de Paiva CS. Reduced corneal innervation in the CD25 null model of Sjogren syndrome. *Int J Mol Sci*. 2018;19:E3821.

35. Stepp MA, Pal-Ghosh S, Tadvalkar G, Williams A, Pflugfelder SC, de Paiva CS. Reduced intraepithelial corneal nerve density and sensitivity accompany desiccating stress and aging in C57BL/6 mice. *Exp Eye Res*. 2018;169:91–98.

36. De Paiva CS, Chotikavanich S, Pangelinan SB, et al. IL-17 disrupts corneal barrier following desiccating stress. *Mucosal Immunol*. 2009;2:243–253.

37. Hosal BM, Ornek N, Zilelioglu G, Elhan AH. Morphology of corneal nerves and corneal sensation in dry eye: a preliminary study. *Eye (Lond)*. 2005;19:1276–1279.

38. Villani E, Galimberti D, Viola F, Mapelli C, Ratiglia R. The cornea in Sjogren's syndrome: an in vivo confocal study. *Invest Ophthalmol Vis Sci*. 2007;48:2017–2022.

39. Villani E, Magnani F, Viola F, et al. In vivo confocal evaluation of the ocular surface morpho-functional unit in dry eye. *Optom Vis Sci*. 2013;90:576–586.

40. Zhang M, Chen J, Luo L, Xiao Q, Sun M, Liu Z. Altered corneal nerves in aqueous tear deficiency viewed by in vivo confocal microscopy. *Cornea*. 2005;24:818–824.

41. Villani E, Galimberti D, Viola F, Mapelli C, Del Papa N, Ratiglia R. Corneal involvement in rheumatoid arthritis: an in vivo confocal study. *Invest Ophthalmol Vis Sci*. 2008;49:560–564.

42. Villani E, Garoli E, Termine V, Pichi F, Ratiglia R, Nucci P. Corneal confocal microscopy in dry eye treated with corticosteroids. *Optom Vis Sci*. 2015;92:e290–e295.

43. Wei Y, Asbell PA. The core mechanism of dry eye disease is inflammation. *Eye Contact Lens*. 2014;40:248–256.

44. Yagci A, Gurdal C. The role and treatment of inflammation in dry eye disease. *Int Ophthalmol*. 2014;34:1291–1301.

45. Tepelus TC, Chiu GB, Huang J, et al. Correlation between corneal innervation and inflammation evaluated with confocal microscopy and symptomatology in patients with dry eye syndromes: a preliminary study. *Graefes Arch Clin Exp Ophthalmol*. 2017;255:1771–1778.

46. Rosenberg ME, Tervo TM, Immonen IJ, Muller LJ, Gronhagen-Riska C, Vesaluoma MH. Corneal structure and sensitivity in type 1 diabetes mellitus. *Invest Ophthalmol Vis Sci*. 2000;41: 2915–2921.

47. Malik RA, Kallinikos P, Abbott CA, et al. Corneal confocal microscopy: a non-invasive surrogate of nerve fibre damage and repair in diabetic patients. *Diabetologia*. 2003;46:683–688.

48. Patel DV, McGhee CN. Mapping the corneal sub-basal nerve plexus in keratoconus by in vivo laser scanning confocal microscopy. *Invest Ophthalmol Vis Sci*. 2006;47:1348–1351.

49. Tuominen IS, Konttinen YT, Vesaluoma MH, Moilanen JA, Helinto M, Tervo TM. Corneal innervation and morphology in primary Sjogren's syndrome. *Invest Ophthalmol Vis Sci*. 2003;44:2545–2549.

50. Xu KP, Yagi Y, Tsubota K. Decrease in corneal sensitivity and change in tear function in dry eye. *Cornea*. 1996;15:235–239.

51. Reichard M, Weiss H, Poletti E, et al. Age-related changes in murine corneal nerves. *Curr Eye Res*. 2016;41:1021–1028.